

---

# AROID: Improving Adversarial Robustness through Online Instance-wise Data Augmentation

---

**Lin Li**

King's College London  
lin.3.li@kcl.ac.uk

**Jianing Qiu**

Imperial College London  
jianing.qiu17@imperial.ac.uk

**Michael Spratling**

King's College London  
michael.spratling@kcl.ac.uk

## Abstract

Deep neural networks are vulnerable to adversarial examples. Adversarial training (AT) is an effective defense against adversarial examples. However, AT is prone to overfitting which degrades robustness substantially. Recently, data augmentation (DA) was shown to be effective in mitigating robust overfitting if appropriately designed and optimized for AT. This work proposes a new method to automatically learn online, instance-wise, DA policies to improve robust generalization for AT. A novel policy learning objective, consisting of Vulnerability, Affinity and Diversity, is proposed and shown to be sufficiently effective and efficient to be practical for automatic DA generation during AT. This allows our method to efficiently explore a large search space for a more effective DA policy and evolve the policy as training progresses. Empirically, our method is shown to outperform or match all competitive DA methods across various model architectures (CNNs and ViTs) and datasets (CIFAR10, SVHN and Imagenette). Our DA policy reinforced vanilla AT to surpass several state-of-the-art AT methods (with baseline DA) in terms of both accuracy and robustness. It can also be combined with those advanced AT methods to produce a further boost in robustness.

## 1 Introduction

Deep neural networks (DNNs) are well known to be vulnerable to infinitesimal yet highly malicious artificial perturbations in their input, i.e., adversarial examples [36]. Thus far, adversarial training (AT) has been the most effective defense against adversarial attacks [3]. AT is typically formulated as a min-max optimization problem:

$$\arg \min_{\theta} \mathbb{E}[\arg \max_{\delta} \mathcal{L}(x + \delta; \theta)] \quad (1)$$

where the inner maximization searches for the perturbation  $\delta$  to maximize the loss, while the outer minimization searches for the model parameters  $\theta$  to minimize the loss on the perturbed examples.

One major issue of AT is that it is prone to overfitting [34, 42]. Unlike in standard training, overfitting in AT, a.k.a. robust overfitting [34], significantly impairs adversarial robustness. Many efforts [10, 22, 43] have been made to understand robust overfitting and mitigate its effect. One promising solution is data augmentation (DA), which is a common technique to prevent standard training from overfitting. However, many studies [13, 33, 34, 43] have revealed that advanced DA methods, originally proposed for standard training, often fail to improve adversarial robustness. Therefore, DA was usually combined with other regularization techniques such as Stochastic Weight Averaging

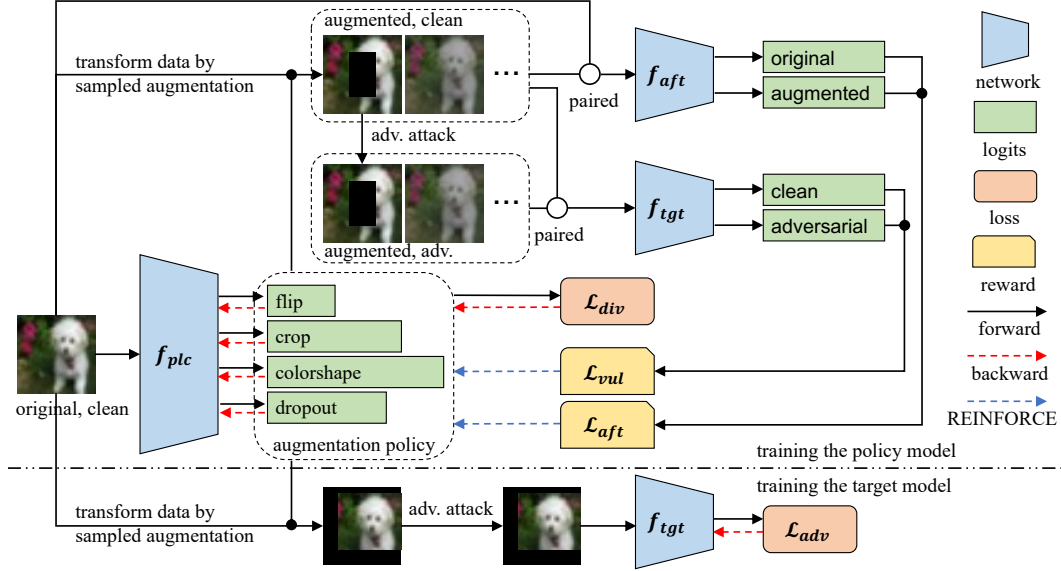


Figure 1: An overview of the proposed method (legend in the right column). The top part shows the pipeline for training the policy model, while the bottom illustrates the pipeline for training the target model. Please refer to Section 3 for a detailed explanation.



Figure 2: An example of the proposed augmentation sampling procedure. The policy model takes an image as input and outputs logit values defining multiple, multinomial, probability distributions corresponding to different sub-policies. A sub-policy code is created by sampling from each of these distributions, and decoded into a sub-policy, i.e., a transformation and its magnitude. These transformations are applied, in sequence, to augment the image.

(SWA) [33], Consistency regularization [37] and Separate Batch Normalization [1] to improve its effectiveness. However, recent work [23] demonstrated that DA alone can significantly improve AT if it has strong diversity and well-balanced hardness. This suggests that standard training and AT may require different DA strategies, especially in terms of hardness. It is thus necessary to design DA schemes dedicated to AT.

IDBH [23] is the first and the latest DA scheme specifically designed for AT. Despite its impressive robust performance, IDBH employs a heuristic search method to manually optimize DA. This search process requires a complete AT for every sampled policy, which induces prohibitive computational cost and scales poorly to large datasets and models. Hence, when the computational budget is limited, the hyperparameters for IDBH might be found using a reduced search space and by employing a smaller model, leading to compromised performance.

Another issue is that IDBH, in common with other conventional DA methods such as AutoAugment [6] and TrivialAugment [31], applies the same strategy to all samples in the dataset throughout training. The distinctions between different training samples, and between the model checkpoints at different stages of training, are neglected. We hypothesize that different data samples at the same stage of training, as well as the same sample at the different stages of training, demand different DAs. Hence, we conjecture that an improvement in robustness could be realized by customizing DA for data samples and training stages.

To address the above issues, this work proposes a bi-level optimization framework (see Fig. 1) to automatically learn Adversarial Robustness by Online Instance-wise Data-augmentation (AROID). To the best of our knowledge, AROID is the first automated DA method specific to AT. AROID employs a multi-head DNN-based policy model to map a data sample to a DA policy (see Fig. 2). This DA policy is defined as a sequence of pre-defined transformations applied with strength determined by the output of the policy model. This policy model is optimized, alongside the training of the target model, towards three novel objectives to achieve a target level of hardness and diversity. DA policies, therefore, are customized for each data instance and evolve with the target network as training progresses. This in practice produces a more globally optimal DA policy and thus benefits robustness. Importantly, the proposed policy learning objectives, in contrast to the conventional ones like validation accuracy [6], do not reserve a subset of the training data for validation and do not rely on prohibitively expensive inner loops for training the target model to evaluate the rewards of the sampled policies. The former ensures the entire training set is available for training to avoid potential data scarcity. The latter enables policy optimization to be much more efficient and scalable so that it is more practical for AT. Compared to IDBH in particular, this allows our approach to explore a larger space of DAs on the target.

Extensive experiments show that AROID outperforms or matches all competitive DA methods across various datasets and model architectures while being more efficient than the prior art IDBH. AROID achieves state-of-the-art robustness for DA methods on the standard benchmarks of CIFAR10 and Imagenette with WideResNets and Vision Transformers, respectively. Furthermore, AROID outperforms, regarding accuracy and robustness, state-of-the-art AT methods. AROID also complements such robust training methods and can be combined with them to improve robustness further.

## 2 Related Work

**Robust training.** To mitigate overfitting in AT, many methods other than DA, have been previously proposed. One line of works, IGR [35], CURE [30], AdvLC [22], discovered a connection between adversarial vulnerability and the smoothness of input loss landscape, and promoted robustness by smoothing the input loss landscape. Meanwhile, We et al. [43] and Chen et al. [4] found that robust generalization can be improved by a flat weight loss landscape and proposed AWP and SWA, respectively, to smooth the weight loss landscape during AT. RWP [44] and SEAT [38] were later proposed to further refine AWP and SWA, respectively, to increase robustness. Many works, including MART [40], LAS-AT [19], ISEAT [21], considered the difference between individual training instances and improved AT through regularizing in an instance-wise manner. Our proposed approach is also instance-wise, but contrary to existing methods tackles robust overfitting via DA instead of robust regularization. As shown in Section 4.2, it works well alone and, more importantly, complements the above techniques.

**Data augmentation for standard training.** Although DA has been a common practice in many fields, we only review vision-based DA in this section as it is most related to our work. In computer vision, DA can be generally categorized as: basic, composite and mixup. Basic augmentations refer to a series of image transformations that can be applied independently. They mainly include crop-based (Random Crop [15], Cropshift [23], etc.), color-based (Brightness, Contrast, etc.), geometric-based (Rotation, Shear, etc.) and dropout-based (Cutout [9], Random Erasing [49], etc.) transformations. Composite augmentations denote the composition of basic augmentations. Augmentations are composed into a single policy/schedule usually through two ways: interpolation [17, 39] and sequencing [6, 7, 31]. Mixup [47], and analogous works like Cutmix [45], can be considered as a special case of interpolation-based composition, which combines a pair of different images, instead of augmentations, as well as their labels to create a new image and its label.

Composite augmentations by design have many hyperparameters to optimize. Most previous works, as well as the pioneering AutoAugment [6], tackled this issue using automated machine learning (AutoML). DA policies were optimized towards maximizing validation accuracy [6, 24, 26, 27], maximizing training loss [48] or matching the distribution density between the original and augmented data [14, 25]. Optimization here is particularly challenging since DA operations are usually non-differentiable. Major solutions seek to estimate the gradient of DA learning objective w.r.t. the policy generator or DA operations using, e.g., policy gradient methods [6, 26, 48] or reparameterization trick [14, 24]. Alternative optimization techniques include Bayesian optimization [25] and population-based training [18]. Noticeably, several works like RandAugment [7] and TrivialAugment [31] found

that if the augmentation space and schedule were appropriately designed, competitive results could be achieved using a simple hyperparameter grid search or fixed hyperparameters. This implies that in standard training these advanced yet complicated methods may not be necessary. However, it remains an open question if simple search can still match these advanced optimization methods in AT. Our method is the first automated DA approach specific for AT. We follow the line of policy gradient methods to enable learning DA policies. A key distinction here is that our policy learning objective is designed to guide the learning of DA policies towards improved robustness for AT, while the objective of the above methods is to increase accuracy for standard training.

### 3 Optimizing Data Augmentation for Adversarial Robustness

We propose a method to automatically learn DA alongside AT to improve robust generalization. An **instance-wise** DA policy is produced by a policy model and learned by optimizing the policy model towards three novel objectives. Updating of the policy model and the target model (the one being adversarially trained for the target task) alternates throughout training (the policy model is updated every  $K$  updates of the target model), yielding an **online** DA strategy. This online, instance-adaptive, strategy produces different augmentations for different data instances at different stages of training.

The following notation is used.  $\mathbf{x} \in \mathbb{R}^d$  is a  $d$ -dimensional sample whose ground truth label is  $y$ .  $\mathbf{x}_i$  refers to  $i$ -th sample in a dataset. The model is parameterized by  $\theta$ .  $\mathcal{L}(\mathbf{x}, y; \theta)$  or  $\mathcal{L}(\mathbf{x}; \theta)$  for short denotes the predictive loss evaluated with  $\mathbf{x}$  w.r.t. the model  $\theta$  (Cross-Entropy loss was used in all experiments).  $\rho(\mathbf{x}; \theta)$  computes the adversarial example of  $\mathbf{x}$  w.r.t. the model  $\theta$ .  $p_i(\mathbf{x}; \theta)$  refers to the output of the Softmax function applied to the final layer of the model, i.e., the probability at  $i$ -th logit given the input  $\mathbf{x}$ .

#### 3.1 Modeling the Data Augmentation Policy using DNNs

Following the design of IDBH [23] and TrivialAugment [31], DA is implemented using four types of transformations: flip, crop, color/shape and dropout applied in order. We implement flip using HorizontalFlip, crop using Cropshift [23], dropout using Erasing<sup>1</sup> [49], and color/shape using a set of operations including Color, Sharpness, Brightness, Contrast, Autocontrast, Equalize, Shear (X and Y), Rotate, Translate (X and Y), Solarize and Posterize. A dummy operation, Identity, is included in each augmentation group to allow data to pass through unchanged. More details including the complete augmentation space are described in Appendix A.

To customize the DA applied to each data instance individually, a policy model parameterized by  $\theta_{plc}$ , is used to produce a DA policy conditioned on the input data (see Fig. 2). The policy model employs a DNN backbone to extract features from the data, and multiple, parallel, linear prediction heads on the top of the extracted features to predict the policy. The policy model used in this work has four heads corresponding to the four types of DA described above<sup>2</sup>. The output of a head is converted into a multinomial distribution where each logit represents a pre-defined sub-policy, i.e., an augmentation operation associated with a strength/magnitude (e.g. ShearX, 0.1). Different magnitudes of the same operation are represented by different logits, so that each has its own chance of being sampled. A particular sequence of sub-policies to apply to the input image are selected based on the probabilities encoded in the four heads of the policy network.

#### 3.2 Objectives for Learning the Data Augmentation Policy

The policy model is trained using three novel objectives: (adversarial) Vulnerability, Affinity and Diversity. Vulnerability [22] measures the loss variation caused by adversarial perturbation on the augmented data w.r.t. the target model:

$$\mathcal{L}_{vul}(\mathbf{x}; \theta_{plc}) = \mathcal{L}(\rho(\hat{\mathbf{x}}; \theta_{tgt}); \theta_{tgt}) - \mathcal{L}(\hat{\mathbf{x}}; \theta_{tgt}), \text{ where } \hat{\mathbf{x}} = \Phi(\mathbf{x}; S(\theta_{plc}(\mathbf{x}))) \quad (2)$$

$\Phi(\mathbf{x}; S(\theta_{plc}(\mathbf{x})))$  augments  $\mathbf{x}$  by  $S(\theta_{plc}(\mathbf{x}))$ , the augmentations sampled from the output distribution of policy model conditioned on  $\mathbf{x}$ , so  $\hat{\mathbf{x}}$  is the augmented data. A larger Vulnerability indicates that  $\mathbf{x}$  becomes more vulnerable to adversarial attack after DA. A common belief about the relationship

<sup>1</sup>Different from the original version applied at half chance, here erasing is always applied but the location and aspect ratio are randomly sampled from the given range.

<sup>2</sup>When training on SVHN only three heads were used, as HorizontalFlip is not appropriate for this dataset.

between training data and robustness is that AT benefits from adversarially hard samples. From a geometric perspective, maximizing Vulnerability encourages the policy model to project data into the previously less-robustified space. Nevertheless, the maximization of Vulnerability, if not constrained, would likely favor those augmentations producing samples far away from the original distribution. Training with such augmentations was observed to degrade accuracy and even robustness if accuracy overly reduced [23]. Therefore, Vulnerability should be maximized while the distribution shift caused by augmentation is constrained:

$$\arg \max_{\theta_{plc}} \mathcal{L}_{vul}(\mathbf{x}; \theta_{plc}) \text{ s.t. } ds(\mathbf{x}, \hat{\mathbf{x}}) \leq D \quad (3)$$

where  $ds(\cdot)$  measures the distribution shift between two samples and  $D$  is a constant. Directly solving Eq. (3) is intractable, so we convert it into an unconstrained optimization problem by adding a penalty on the distribution shift as:

$$\arg \max_{\theta_{plc}} \mathcal{L}_{vul}(\mathbf{x}; \theta_{plc}) - \lambda \cdot ds(\mathbf{x}, \hat{\mathbf{x}}) \quad (4)$$

where  $\lambda$  is a hyperparameter and a larger  $\lambda$  corresponds to a tighter constraint on distribution shift, i.e., smaller  $D$ . Distribution shift is measured using a variant of the Affinity metric [12]:

$$ds(\mathbf{x}, \hat{\mathbf{x}}) = \mathcal{L}_{aft}(\mathbf{x}; \theta_{plc}) = \mathcal{L}(\hat{\mathbf{x}}; \theta_{aft}) - \mathcal{L}(\mathbf{x}; \theta_{aft}) \quad (5)$$

Affinity captures the loss variation caused by DA w.r.t. a model  $\theta_{aft}$  (called the affinity model): a model pre-trained on the original data (i.e., without any data augmentation). Affinity increases as the augmentation proposed by the policy network makes data harder for the affinity model to correctly classify. By substituting Eq. (5) into Eq. (4), we obtain an adjustable Hardness objective:

$$\mathcal{L}_{hrd}(\mathbf{x}; \theta_{plc}) = \mathcal{L}_{vul}(\mathbf{x}; \theta_{plc}) - \lambda \cdot \mathcal{L}_{aft}(\mathbf{x}; \theta_{plc}) \quad (6)$$

This encourages the DA produced by the policy model to be at a level of hardness defined by  $\lambda$  (larger values of  $\lambda$  corresponding to lower hardness). Ideally,  $\lambda$  should be tuned to ensure the distribution shift caused by DA is sufficient to benefit robustness while not being so severe as to harm accuracy.

Last, we introduce a Diversity objective to promote diverse DA. Diversity enforces a relaxed uniform distribution prior over the logits of the policy model, i.e., the output augmentation distribution:

$$\mathcal{L}_{div}^h(\mathbf{x}) = \frac{1}{C} \left[ - \sum_i^{p_i^h < l} \log(p_i^h(\mathbf{x}; \theta_{plc})) + \sum_j^{p_j^h > u} \log(p_j^h(\mathbf{x}; \theta_{plc})) \right] \quad (7)$$

$C$  is the total count of logits violating either lower ( $l$ ), or upper ( $u$ ) limits and  $h$  is the index of the prediction head. Intuitively speaking, the Diversity loss penalizes overly small and large probabilities, helping to constrain the distribution to lie in a pre-defined range ( $l, u$ ). As  $l$  and  $u$  approach the mean probability, the enforced prior becomes closer to a uniform distribution, which corresponds to a highly diverse DA policy. Diversity encourages the policy model to avoid the over-exploitation of certain augmentations and to explore other candidate augmentations. Note that Diversity is applied to the color/shape head in a hierarchical way: type-wise and strength-wise inside each type of augmentation.

Combining the above three objectives together, the policy model is trained to optimize:

$$\arg \min_{\theta_{plc}} -\mathbb{E}_{i \in B} \mathcal{L}_{hrd}(\mathbf{x}_i; \theta_{plc}) + \beta \cdot \mathbb{E}_{h \in H} \mathcal{L}_{div}^h(\mathbf{x}; \theta_{plc}) \quad (8)$$

where  $B$  is the batch size and  $\beta$  trades-off hardness against diversity.  $\mathcal{L}_{div}^h$  is calculated across instances in a batch, so no need for averaging over  $B$  like  $\mathcal{L}_{hrd}$ . The design of Eq. (8) reflects the prior that DA should have strong diversity and well-balanced hardness to be effective for AT [23].

### 3.3 Optimization

The entire training is a bi-level optimization process (Algo. 1): the target and policy models are updated alternately. This online training strategy adapts the policy model to the varying demands for DA from the target model at the different stages of training. The target model is optimized using AT with the augmentation sampled from the policy model:

$$\arg \min_{\theta_{tgt}} \mathcal{L}(\rho(\Phi(\mathbf{x}; S(\theta_{plc}(\mathbf{x}))); \theta_{tgt}); \theta_{tgt}) \quad (9)$$

---

**Algorithm 1.** High-level training procedures of the proposed method.  $\alpha$  is the learning rate.  $M$  is the number of training iterations.

---

```

for  $i = 1$  to  $M$  do
  // for every  $K$  iterations
  if  $i \% K == 0$  then
    // update the policy model
    // by Algo. 2
  end
  // the policy distribution
   $d = \theta_{plc}(\mathbf{x}_i)$ 
  // sample & apply augmentations
   $\hat{\mathbf{x}}_i = \Phi(\mathbf{x}_i; S(d))$ 
   $L = \mathcal{L}(\rho(\hat{\mathbf{x}}_i; \theta_{tgt}); \theta_{tgt})$ 
  // update the target model
   $\theta_{tgt} = \theta_{tgt} - \alpha_{tgt} \cdot \nabla_{\theta_{tgt}} L$ 
end

```

---



---

**Algorithm 2.** Pseudo code of training the policy model for one iteration.  $\mathbf{x}$  is randomly sampled from the entire dataset.

---

```

 $d = \theta_{plc}(\mathbf{x})$ 
// same  $\mathbf{x}$  used by all trajectories
for  $t = 1$  to  $T$  do
   $\hat{\mathbf{x}}^{(t)} = \Phi(\mathbf{x}, S(d))$ 
   $\mathcal{P}^{(t)} = \prod_{h=1}^H p^{(t)h}$  // prob of traj  $t$ 
   $\mathcal{L}_{hrd}^{(t)}$  // computed using Eq. (6)
end
 $\tilde{\mathcal{L}}_{hrd} = \frac{1}{T} \sum_{t=1}^T \mathcal{L}_{hrd}^{(t)}$  // mean  $\mathcal{L}_{hrd}^{(t)}$ 
 $L = \frac{1}{T} \sum_{t=1}^T \log(\mathcal{P}^{(t)}) [\mathcal{L}_{hrd}^{(t)} - \tilde{\mathcal{L}}_{hrd}]$ 
 $\mathcal{L}_{div}^{(h)}$  // computed using Eq. (7)
 $L = -L + \beta \frac{1}{H} \sum_{h=1}^H \mathcal{L}_{div}^{(h)}$ 
 $\theta_{plc} = \theta_{plc} - \alpha_{plc} \cdot \nabla_{\theta_{plc}} L$ 

```

---

After every  $K$  updates of the target model, the policy model is updated using the gradients of the policy learning loss as follows:

$$\frac{Eq. (8)}{\partial \theta_{plc}} = -\frac{\partial \mathbb{E}_{i \in B} \mathcal{L}_{hrd}(\mathbf{x}_i; \theta_{plc})}{\partial \theta_{plc}} + \beta \frac{\mathbb{E}_{h \in H} \mathcal{L}_{div}^h(\mathbf{x}; \theta_{plc})}{\partial \theta_{plc}} \quad (10)$$

The latter can be derived directly, while the former  $\frac{\partial \mathcal{L}_{hrd}}{\partial \theta_{plc}}$  cannot because the involved augmentation operations are non-differentiable. To estimate these gradients, we apply the REINFORCE algorithm [41] with baseline trick to reduce the variance of gradient estimation. It first samples  $T$  augmentations, named trajectories, in parallel from the policy model and then computes the real Hardness value,  $\mathcal{L}_{hrd}^{(t)}$ , using Eq. (6) independently on each trajectory  $t$ . The gradients are estimated (see Appendix B for derivation) as follows:

$$\frac{\partial \mathbb{E}_{i \in B} \mathcal{L}_{hrd}(\mathbf{x}_i; \theta_{plc})}{\partial \theta_{plc}} \approx \frac{1}{B \cdot T} \sum_{i=1}^B \sum_{t=1}^T \sum_{h=1}^H \frac{\partial \log(p_{(t)}^h(\mathbf{x}_i; \theta_{plc}))}{\partial \theta_{plc}} [\mathcal{L}_{hrd}^{(t)}(\mathbf{x}_i; \theta_{plc}) - \tilde{\mathcal{L}}_{hrd}] \quad (11)$$

$p_{(t)}^h$  is the probability of the sampled sub-policy at the  $h$ -th head and  $\tilde{\mathcal{L}}_{hrd} = \frac{1}{T} \sum_{t=1}^T \mathcal{L}_{hrd}^{(t)}(\mathbf{x}_i; \theta_{plc})$  is the mean  $\mathcal{L}_{hrd}$  (the baseline used in the baseline trick) averaged over the trajectories. Algo. 2 illustrates one iteration of updating the policy model. Note that, when one model is being updated, backpropagation is blocked through the other. The affinity model, used in calculating the Affinity metric, is fixed throughout training.

## 4 Experiments

The experiments in this section were based on the following setup unless otherwise specified. We evaluated our method on three datasets: CIFAR10 [20], Imagenette<sup>3</sup> and SVHN [32]. We used model architectures WideResNet34-10 (WRN34-10) [46], Vision Transformer (ViT-B/16) [11] and PreAct ResNet-18 (PRN18) [16] respectively for the three datasets. We used the standard training setting specified in [29, 43]. We used  $\ell_\infty$  PGD10 for AT and AutoAttack [5] for evaluating adversarial robustness. Please refer to Appendix C for the detailed experimental settings.

### 4.1 Benchmarking Data Augmentation on Adversarial Robustness

Tab. 1 compares our proposed method against existing DA methods. On CIFAR10 our method outperforms the previous best method, IDBH, in terms of both accuracy and robustness. On Imagenette

---

<sup>3</sup>Imagenette is a subset of ImageNet [8] consisting of 10 classes. We adopt a previous version (v1), <https://s3.amazonaws.com/fast-ai-imageclas/imagenette.tgz>, as suggested by [29].

Table 1: Comparison of the performance of various DA methods. The **best** and **second best** results are highlighted in each column. The baseline augmentation was Horizontal Flip plus Random Crop on CIFAR10 and Imagenette, and None on SVHN.

DA method	CIFAR10 + WRN34-10		Imagenette + ViT-B/16		SVHN + PRN18	
	Accuracy	Robustness	Accuracy	Robustness	Accuracy	Robustness
baseline	85.83±.76	52.26±.02	92.73±.42	66.47±.83	90.54±.74	47.56±.71
Cutout [9]	86.95±.16	52.89±.29	93.27±.31	67.20±.87	90.69±.51	50.88±.45
Cutmix [45]	86.88±.46	53.38±.28	93.87±.61	70.20±.40	91.13±.25	51.95±.40
AutoAugment [6]	87.71±.32	54.60±.33	95.13±.85	67.60±.42	93.68±.17	54.15±.06
TrivialAugment [31]	87.35±.48	53.86±.21	<b>95.25±.99</b>	69.00±.93	93.44±.37	52.78±.26
IDBH [23]	88.61±.17	55.29±.11	95.20±.40	69.93±.31	<b>93.70±.13</b>	<b>54.56±.29</b>
AROID (ours)	<b>88.99±.24</b>	<b>55.91±.25</b>	94.88±.67	<b>71.32±.64</b>	93.30±.17	54.49±.18

our method has significantly higher robustness than the previous best method, Cutmix, while also outperforming that method in terms of accuracy. On SVHN our method achieves a similar robustness to the best existing method, IDBH, with slightly worse accuracy. The slightly better performance of IDBH on SVHN compared to AROID is likely due to the hyperparameters for IDBH having been tuned on the target model, whereas the hyperparameters for IDBH on the other datasets were tuned on a simplified proxy model (PRN18) due to the computational cost of using the target model. This highlights an advantage of AROID over IDBH: an improved efficiency leading to a more effective DA policy tuned to the target network (further discussed in Section 4.5).

It is also worth noting the superiority of our method over Cutmix for ViTs on Imagenette. This contradicts the previous observation that ViTs favor Cutmix and Mixup augmentations [29] and proves that composite DA can beat Mixup-style DA if sufficiently optimized. Lastly, we observed that for ViT-B/16 on Imagenette with the adopted training setting [29], AT particularly with certain DAs like TrivialAugment was less stable showing higher standard deviation in accuracy and/or robustness compared to how they performed on the other two training settings. Nevertheless, this does not affect our conclusion on the AROID’s superiority over others given the evident margin of robustness boost. Investigating the reasons behind the observed instability and designing a new, more stable, training receipt is beyond the scope of this work.

In summary, the proposed method produces higher accuracy and robustness compared to the majority of the alternative DA based methods, and produces state-of-the-art robustness for two datasets. The proposed method also improves on the baseline by a substantial margin for all datasets. This suggests that the proposed method has a good generalization ability across various datasets (low and high resolution) and model architectures (CNNs and ViTs, small and large capacity).

## 4.2 Comparison with State-of-the-art Robust Training Methods

Tab. 2 compares our method against state-of-the-art robust training methods. It can be seen that AROID substantially improves vanilla AT in terms of accuracy (by 3.16%) and robustness (by 3.65%). This improvement is sufficient to boost the performance of vanilla AT to surpass the state-of-the-art robust training methods like SEAT and LAS-AWP in terms of both accuracy and robustness. This suggests that our method achieved a better trade-off between accuracy and robustness while boosting robustness. More importantly, our method, as it is based on DA, can be easily integrated into the pipeline of existing robust training methods and, as our results show, is complementary to them. By combining with SWA and/or AWP, our method substantially improves robustness even further while still maintaining an accuracy higher than that achieved by others methods.

## 4.3 Transferability of Learned Data Augmentation Policy

One limitation of AROID is that the policy model is retrained every time a new target model is trained. This section considers the possibility of enhancing AT by sampling DA policies from pre-trained policy models. This transferred version of AROID is called AROID-T. At each epoch of training the target network, AROID-T uses a policy network checkpoint saved at the corresponding epoch when using AROID. We consider the case where AROID-T is used to train a target network with the same architecture on the same dataset as was used when creating the policy network checkpoints. We

Table 2: The performance of various robust training (RT) methods with baseline (HorizontalFlip+RandomCrop) and our augmentations for WRN34-10 on CIFAR10.

RT method	DA method	Accuracy	Robustness
AT [28]	baseline	85.83±.76	52.26±.02
AT-SWA [33]	baseline	84.30±.14	54.29±.15
AT-AWP [43]	baseline	85.93±.25	54.34±.40
AT-RWP [44]	baseline	86.86 ±.51	54.61±.11
MART [40]	baseline	84.17	51.10
MART-AWP [43]	baseline	84.43	54.23
SEAT [38]	baseline	86.44±.12	55.67±.22
LAS-AT [19]	baseline	86.23	53.58
LAS-AWP [19]	baseline	87.74	55.52
AT [28]	AROID (ours)	<b>88.99±.24</b>	<b>55.91±.25</b>
AT-SWA	AROID (ours)	87.84±.16	56.67±.21
AT-AWP	AROID (ours)	87.94±.11	56.98±.20
AT-AWP-SWA	AROID (ours)	<b>88.39±.10</b>	<b>57.03±.01</b>

Table 3: The performance of our method when the policy model is pre-trained (AROID-T) or trained on-the-fly (AROID) for WRN34-10 on CIFAR10.

Policy source	Accuracy	Robustness
AROID-T	88.76 ± .14	55.61 ± .14
AROID	<b>88.99 ± .24</b>	<b>55.91 ± .25</b>

Table 4: The contribution of each policy learning objective to the performance of our method.  $K = 5$  and  $T = 8$ .

Objective	Accuracy	Robustness
AROID	<b>84.68 ± .15</b>	<b>50.57 ± .13</b>
- Vulnerability	83.97 ± .66	50.41 ± .11
- Affinity	82.40 ± .44	49.72 ± .12
- Diversity	73.88 ± 3.8	22.47 ± 18.9

did not test the transferability across different training setups such as model architectures and robust training methods, because it is expected that the required DA policies will differ, especially when the capacity of the target model is considerably different [23].

As shown in Tab. 3, AROID-T achieved a robustness of 55.61% which is slightly lower than that of AROID (55.91%). Note that the result of AROID-T is still better than that of the previous best DA-based method (IDBH 55.29%, see Tab. 1), and is close to the result of the best robust training method (SEAT 55.67%, see Tab. 2). Therefore, the policy learned by AROID is able to transfer to a reasonable degree, at least when using the same architecture and training settings.

#### 4.4 Ablation Study

This section tests the sensitivity of our method to its hyperparameters and objective design. The experiments were conducted on CIFAR10 using the setup specified at the beginning of Section 4 except that PRN18 was used. By default, AROID was trained with  $\lambda = 0.3$ ,  $\beta = 0.8$  and a Diversity limit of ( $l = 0.9$ ,  $u = 4.0$ ) (see Tab. 7 for an explanation) in this section.

**Policy update frequency  $K$ .** Fig. 3 shows that the highest accuracy and robustness were achieved when  $K = 5$ , i.e., the lowest frequency under the test. This implies that AT benefits from a more "up-to-date" DA. Furthermore, it seems possible to trade accuracy for efficiency by setting a larger  $K$  (up to 20) while maintaining similarly high robustness. In general, the accuracy and robustness of our method declines with lower policy update frequency.

**Number of trajectories  $T$ .** Fig. 4 shows that  $T = 8$  achieved the best trade-off between accuracy and robustness. Accuracy and robustness are high for  $T \geq 6$  and  $T \geq 4$ , respectively. This suggests that (1) there is a minimum requirement on the amount of trajectories for our policy gradient estimator to be accurate and (2) our method may not benefit from increasing  $T$  beyond 8.

**Policy learning objectives.** Each of the three proposed policy learning objectives were removed to evaluate its contribution to AROID's performance. As shown in Tab. 4, removing any of them observably degraded both accuracy and robustness and increased the standard deviation in the accuracy produced in different runs. This suggests that each objective plays an important role in our method. Training the policy network failed without Diversity as the output policy distribution concentrated

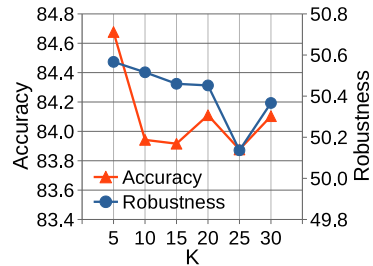


Figure 3: The sensitivity of the performance of AROID w.r.t.  $K$ .  $T = 8$  for all  $K$ .

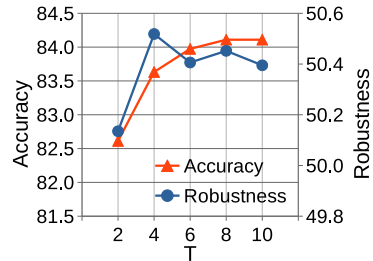


Figure 4: The sensitivity of the performance of AROID w.r.t.  $T$ .  $K = 20$  for all  $T$ .



Table 5: The efficiency comparison between IDBH and AROID with different  $K$  and  $T$  for PRN18 on CIFAR10. The size of search space counts the possible combinations of probabilities and magnitudes. Our search space is uncountable due to its continuous range of probability, but is still greatly larger than that of IDBH since it covers a much wider range of probabilities and magnitudes. Time denotes the total hours required for one search over the search space using an Nvidia A100 GPU.

Method	K	T	Accuracy	Robustness	Search Space			Time
					Probability	Magnitude	Size	
IDBH	-	-	84.23	50.47	discrete	discrete	80	412.83
AROID	5	8	<b>84.68</b>	<b>50.57</b>	continuous	discrete	uncountable	9.51
AROID	20	8	84.11	50.45	continuous	discrete	uncountable	6.85
AROID	20	4	83.63	<u>50.52</u>	continuous	discrete	uncountable	<b>6.24</b>

on several sub-policies, i.e., gave zero probabilities at the remaining sub-policies. The REINFORCE method failed to recover from this situation because it no longer explored other opportunities. Note that the contribution of each objective, esp. Vulnerability and Affinity, can differ considerably across different training settings as the appropriate level of hardness will change.

#### 4.5 Efficiency Comparison

This section compares AROID against IDBH, the only other DA method specifically designed for AT, in terms of efficiency. Before comparison, it is important to be aware that the search cost for IDBH increases linearly with the size of search space, while the cost of AROID stays approximately constant. IDBH thus uses a reduced search space that is greatly smaller than the search space of AROID. Scaling IDBH to this larger search space is intractable, and it would be even more intractable if IDBH was applied to find DAs for each data instance at each stage of training like AROID. Nevertheless, as shown in Tab. 5, a complete search by IDBH over its reduced space is still more costly than our learning-based search over its uncountable (continuous) space. The computational efficiency of AROID can be increased by reducing the policy update frequency (increasing  $K$ ) and/or decreasing the number of trajectories  $T$ , while still matching the robustness of IDBH. Furthermore, the search space of IDBH is simplified based on prior knowledge about the training datasets, which may not generalize to other datasets. One limitation of AROID is that, for efficiency, it optimizes an objective (Eq. (8)) that is a proxy for the true objective (maximizing the validation set robustness). This introduces a few extra hyperparameters that need to be optimized. Nevertheless, our results suggest this can be accelerated by first searching with a cheap setting like  $K = 20$  and  $T = 4$  and then transferring the found values to the final setting, i.e.,  $K = 5$  and  $T = 8$ .

#### 4.6 Visualization of Learned Data Augmentation Policies

The learned DA policies are visualized in Appendix D. We observe that the learned DA policies vary among instances and evolve during training. Furthermore, the augmentation preference of the learned DA policies is consistent to the previous findings [6, 33], which verifies AROID’s effectiveness.

### 5 Conclusion

This work introduces an approach, dubbed AROID, to efficiently learn online, instance-wise, DA policies for improved robust generalization in AT. AROID is the first automated DA method specific for AT. Extensive experiments show its superiority over both alternative DA methods and contemporary AT methods in terms of accuracy and robustness. This confirms the necessity of optimizing DA for improved adversarial robustness. The learned DA policies are visualized to verify the effectiveness of AROID and understand the preference of AT for DA.

However, AROID has some limitations as well. First, despite being more efficient than IDBH, it still adds extra computational burden to training, unless AROID-T is used. This could harm its scalability to larger datasets and model architectures. Second, the Diversity objective enforces a minimal chance (set by the lower limit) of applying harmful transformations and/or harmful magnitudes if they are included in the search space. This constrains the ability of AROID to explore a wider (less filtered)

search space. Future works could investigate more efficient AutoML algorithms for learning DA policies for AT, and design new policy learning objectives to reduce the number of hyperparameters and alleviate the side-effect of Diversity.

## Acknowledgments

The authors acknowledge the use of the research computing facility at King’s College London, King’s Computational Research, Engineering and Technology Environment (CREATE), and the Joint Academic Data science Endeavour (JADE) facility. This research was funded by the King’s - China Scholarship Council (K-CSC).

## References

- [1] S. Addepalli, S. Jain, and V. B. Radhakrishnan. Efficient and Effective Augmentation Strategy for Adversarial Training. In *Advances in Neural Information Processing Systems*, Oct. 2022.
- [2] M. Andriushchenko and N. Flammarion. Understanding and Improving Fast Adversarial Training. In *Advances in Neural Information Processing Systems*, page 12, 2020.
- [3] A. Athalye, N. Carlini, and D. Wagner. Obfuscated Gradients Give a False Sense of Security: Circumventing Defenses to Adversarial Examples. In *International Conference on Machine Learning*, July 2018.
- [4] T. Chen, Z. Zhang, S. Liu, S. Chang, and Z. Wang. Robust Overfitting may be mitigated by properly learned smoothening. In *International Conference on Learning Representations*, 2021.
- [5] F. Croce and M. Hein. Reliable Evaluation of Adversarial Robustness with an Ensemble of Diverse Parameter-free Attacks. In *Proceedings of the 37th International Conference on Machine Learning*, page 11, 2020.
- [6] E. D. Cubuk, B. Zoph, D. Mane, V. Vasudevan, and Q. V. Le. AutoAugment: Learning Augmentation Strategies From Data. In *2019 IEEE/CVF Conference on Computer Vision and Pattern Recognition (CVPR)*, pages 113–123, Long Beach, CA, USA, June 2019. IEEE.
- [7] E. D. Cubuk, B. Zoph, J. Shlens, and Q. V. Le. Randaugment: Practical automated data augmentation with a reduced search space. In *Advances in Neural Information Processing Systems*, 2020.
- [8] J. Deng, W. Dong, R. Socher, L. Li, Kai Li, and Li Fei-Fei. ImageNet: A large-scale hierarchical image database. In *2009 IEEE Conference on Computer Vision and Pattern Recognition*, pages 248–255, June 2009. ISSN: 1063-6919.
- [9] T. DeVries and G. W. Taylor. Improved Regularization of Convolutional Neural Networks with Cutout. *arXiv:1708.04552 [cs]*, Nov. 2017. arXiv: 1708.04552.
- [10] Y. Dong, K. Xu, X. Yang, T. Pang, Z. Deng, H. Su, and J. Zhu. Exploring Memorization in Adversarial Training. In *International Conference on Learning Representations*, 2022.
- [11] A. Dosovitskiy, L. Beyer, A. Kolesnikov, D. Weissenborn, X. Zhai, T. Unterthiner, M. Dehghani, M. Minderer, G. Heigold, S. Gelly, J. Uszkoreit, and N. Houlsby. An Image is Worth 16x16 Words: Transformers for Image Recognition at Scale. In *International Conference on Learning Representations*, 2021.
- [12] R. Gontijo-Lopes, S. Smullin, E. D. Cubuk, and E. Dyer. Tradeoffs in Data Augmentation: An Empirical Study. In *International Conference on Learning Representations*, 2021.
- [13] S. Gowal, C. Qin, J. Uesato, T. Mann, and P. Kohli. Uncovering the Limits of Adversarial Training against Norm-Bounded Adversarial Examples. *arXiv:2010.03593 [cs, stat]*, Mar. 2021. arXiv: 2010.03593.

- [14] R. Hataya, J. Zdenek, K. Yoshizoe, and H. Nakayama. Faster AutoAugment: Learning Augmentation Strategies Using Backpropagation. In A. Vedaldi, H. Bischof, T. Brox, and J.-M. Frahm, editors, *Computer Vision – ECCV 2020*, Lecture Notes in Computer Science, pages 1–16, Cham, 2020. Springer International Publishing.
- [15] K. He, X. Zhang, S. Ren, and J. Sun. Deep Residual Learning for Image Recognition. In *2016 IEEE Conference on Computer Vision and Pattern Recognition (CVPR)*, pages 770–778, Las Vegas, NV, USA, June 2016. IEEE.
- [16] K. He, X. Zhang, S. Ren, and J. Sun. Identity Mappings in Deep Residual Networks. In *Proceedings of the European Conference on Computer Vision (ECCV)*, 2016.
- [17] D. Hendrycks\*, N. Mu\*, E. D. Cubuk, B. Zoph, J. Gilmer, and B. Lakshminarayanan. AugMix: A Simple Data Processing Method to Improve Robustness and Uncertainty. In *International Conference on Learning Representations*, 2020.
- [18] D. Ho, E. Liang, X. Chen, I. Stoica, and P. Abbeel. Population Based Augmentation: Efficient Learning of Augmentation Policy Schedules. In *Proceedings of the 36th International Conference on Machine Learning*, pages 2731–2741. PMLR, May 2019. ISSN: 2640-3498.
- [19] X. Jia, Y. Zhang, B. Wu, K. Ma, J. Wang, and X. Cao. LAS-AT: Adversarial Training With Learnable Attack Strategy. In *Proceedings of the IEEE/CVF Conference on Computer Vision and Pattern Recognition*, pages 13398–13408, 2022.
- [20] A. Krizhevsky. Learning multiple layers of features from tiny images. Technical report, 2009.
- [21] L. Li and M. Spratling. Improved Adversarial Training Through Adaptive Instance-wise Loss Smoothing, Mar. 2023. arXiv:2303.14077 [cs].
- [22] L. Li and M. Spratling. Understanding and combating robust overfitting via input loss landscape analysis and regularization. *Pattern Recognition*, 136:109229, Apr. 2023.
- [23] L. Li and M. W. Spratling. Data augmentation alone can improve adversarial training. In *The Eleventh International Conference on Learning Representations*, Feb. 2023.
- [24] Y. Li, G. Hu, Y. Wang, T. Hospedales, N. M. Robertson, and Y. Yang. Differentiable Automatic Data Augmentation. In A. Vedaldi, H. Bischof, T. Brox, and J.-M. Frahm, editors, *Computer Vision – ECCV 2020*, pages 580–595, Cham, 2020. Springer International Publishing.
- [25] S. Lim, I. Kim, T. Kim, C. Kim, and S. Kim. Fast AutoAugment. In *Advances in Neural Information Processing Systems*, volume 32. Curran Associates, Inc., 2019.
- [26] C. Lin, M. Guo, C. Li, X. Yuan, W. Wu, J. Yan, D. Lin, and W. Ouyang. Online Hyper-Parameter Learning for Auto-Augmentation Strategy. In *2019 IEEE/CVF International Conference on Computer Vision (ICCV)*, pages 6578–6587, Oct. 2019. ISSN: 2380-7504.
- [27] A. Liu, Z. Huang, Z. Huang, and N. Wang. Direct Differentiable Augmentation Search. In *Proceedings of the IEEE/CVF International Conference on Computer Vision*, pages 12219–12228, 2021.
- [28] A. Madry, A. Makelov, L. Schmidt, D. Tsipras, and A. Vladu. Towards Deep Learning Models Resistant to Adversarial Attacks. In *International Conference on Learning Representations*, 2018.
- [29] Y. Mo, D. Wu, Y. Wang, Y. Guo, and Y. Wang. When Adversarial Training Meets Vision Transformers: Recipes from Training to Architecture. In *Advances in Neural Information Processing Systems*, Oct. 2022.
- [30] S.-M. Moosavi-Dezfooli, A. Fawzi, J. Uesato, and P. Frossard. Robustness via Curvature Regularization, and Vice Versa. In *Proceedings of the IEEE/CVF Conference on Computer Vision and Pattern Recognition*, pages 9078–9086, 2019.
- [31] S. G. Müller and F. Hutter. TrivialAugment: Tuning-Free Yet State-of-the-Art Data Augmentation. In *Proceedings of the IEEE/CVF International Conference on Computer Vision*, pages 774–782, 2021.

- [32] Y. Netzer, T. Wang, A. Coates, A. Bissacco, B. Wu, and A. Y. Ng. Reading Digits in Natural Images with Unsupervised Feature Learning. In *NIPS Workshop on Deep Learning and Unsupervised Feature Learning 2011*, 2011.
- [33] S.-A. Rebuffi, S. Gowal, D. A. Calian, F. Stimberg, O. Wiles, and T. Mann. Data Augmentation Can Improve Robustness. In *Neural Information Processing Systems*, May 2021.
- [34] L. Rice, E. Wong, and J. Z. Kolter. Overfitting in adversarially robust deep learning. In *Proceedings of the 37th International Conference on Machine Learning*, page 12, 2020.
- [35] A. S. Ross and F. Doshi-Velez. Improving the Adversarial Robustness and Interpretability of Deep Neural Networks by Regularizing their Input Gradients. In *AAAI Conference on Artificial Intelligence*, page 10, 2018.
- [36] C. Szegedy, W. Zaremba, I. Sutskever, J. Bruna, D. Erhan, I. Goodfellow, and R. Fergus. Intriguing properties of neural networks. In *International Conference on Learning Representations*, 2014.
- [37] J. Tack, S. Yu, J. Jeong, M. Kim, S. J. Hwang, and J. Shin. Consistency Regularization for Adversarial Robustness. *Proceedings of the AAAI Conference on Artificial Intelligence*, 36(8):8414–8422, June 2022.
- [38] H. Wang and Y. Wang. Self-ensemble Adversarial Training for Improved Robustness. In *International Conference on Learning Representations*, May 2022.
- [39] H. Wang, C. Xiao, J. Kossaifi, Z. Yu, A. Anandkumar, and Z. Wang. AugMax: Adversarial Composition of Random Augmentations for Robust Training. In *Thirty-Fifth Conference on Neural Information Processing Systems*, May 2021.
- [40] Y. Wang, D. Zou, J. Yi, J. Bailey, X. Ma, and Q. Gu. Improving Adversarial Robustness Requires Revisiting Misclassified Examples. In *International Conference on Learning Representations*, page 14, 2020.
- [41] R. J. Williams. Simple statistical gradient-following algorithms for connectionist reinforcement learning. *Machine Learning*, 8(3):229–256, May 1992.
- [42] E. Wong, L. Rice, and J. Z. Kolter. Fast is better than free: Revisiting adversarial training. In *International Conference on Learning Representations*, 2020.
- [43] D. Wu, S.-T. Xia, and Y. Wang. Adversarial Weight Perturbation Helps Robust Generalization. In *Advances in Neural Information Processing Systems*, volume 33, pages 2958–2969, 2020.
- [44] C. Yu, B. Han, M. Gong, L. Shen, S. Ge, D. Bo, and T. Liu. Robust Weight Perturbation for Adversarial Training. In *Thirty-First International Joint Conference on Artificial Intelligence*, volume 4, pages 3688–3694, July 2022. ISSN: 1045-0823.
- [45] S. Yun, D. Han, S. J. Oh, S. Chun, J. Choe, and Y. Yoo. CutMix: Regularization Strategy to Train Strong Classifiers With Localizable Features. In *Proceedings of the IEEE/CVF International Conference on Computer Vision*, pages 6023–6032, 2019.
- [46] S. Zagoruyko and N. Komodakis. Wide Residual Networks. In *Proceedings of the British Machine Vision Conference 2016*, pages 87.1–87.12, York, UK, 2016. British Machine Vision Association.
- [47] H. Zhang, M. Cisse, Y. N. Dauphin, and D. Lopez-Paz. mixup: Beyond Empirical Risk Minimization. In *International Conference on Learning Representations*, Feb. 2018.
- [48] X. Zhang, Q. Wang, J. Zhang, and Z. Zhong. Adversarial AutoAugment. In *International Conference on Learning Representations*, 2020.
- [49] Z. Zhong, L. Zheng, G. Kang, S. Li, and Y. Yang. Random Erasing Data Augmentation. In *Proceedings of the AAAI Conference on Artificial Intelligence*, volume 34, pages 13001–13008, Apr. 2020. Number: 07.

Table 6: Augmentation space

Flip			Crop			Color/Shape			Dropout		
operations	magnitudes	count	operations	magnitudes	count	operations	magnitudes	count	operations	magnitudes	count
Identity	-	1	Identity	-	1	Identity	-	1	Identity	-	1
Horiz. Flip	-	1	Cropshift	1, 2, 3, 4, 5, 6, 7, 8, 9, 10, 11, 12, 13, 14, 15	15	Autocontrast	-	1	Erasing	.05, .10, .15, .20, .25, .30, .35, .40, .45, .50	10
						Equalize	-	1			
						Posterize	4, 5, 6, 7, 8	5			
						Solarize	25, 51, 76, 102, 128, 153, 179, 204, 230, 256	10			
						Rotate	3, 6, 9, 12, 15, 18, 21, 24, 27, 30	10			
						ShearX	.03, .06, .09, .12, .15, .18, .21, .24, .27, .30	10			
						ShearY	.03, .06, .09, .12, .15, .18, .21, .24, .27, .30	10			
						TranslateX	1, 2, 3, 4, 5, 6, 7, 8, 9, 10	10			
						TranslateY	1, 2, 3, 4, 5, 6, 7, 8, 9, 10	10			
						Color	.28, .46, .64, .82, 1.0, 1.18, 1.36, 1.54, 1.72, 1.9	10			
						Contrast	.28, .46, .64, .82, 1.0, 1.18, 1.36, 1.54, 1.72, 1.9	10			
						Brightness	.28, .46, .64, .82, 1.0, 1.18, 1.36, 1.54, 1.72, 1.9	10			
						Sharpness	.28, .46, .64, .82, 1.0, 1.18, 1.36, 1.54, 1.72, 1.9	10			

## A DA Search Space for AROID

Tab. 6 shows the complete DA search space used by AROID. For Color/Shape group, we adopted the same operations as RandAugment’s, but discretize the range of magnitudes for each operation into 10 even values if possible. For Erasing in Dropout group, the magnitude corresponds to the scale (the proportion of erased area against input image), while the aspect ratio (of erased area) is uniformly sampled from range (0.3, 3.3). The search space only defines the operations and their magnitudes, while the probabilities of applying these operations are learned by AROID.

## B Detailed Derivation

This section discusses how we derive the gradients of Hardness metric w.r.t. the parameters of the policy model:

$$\frac{\partial \mathbb{E}_{i \in B} \mathcal{L}_{hrd}(\mathbf{x}_i; \boldsymbol{\theta}_{plc})}{\partial \boldsymbol{\theta}_{plc}} \quad (12)$$

First, we rewrite Eq. (12) as below, so that we can focus on the gradient derivation part.

$$\frac{1}{B} \sum_{i=1}^B \frac{\partial \mathcal{L}_{hrd}(\mathbf{x}_i; \boldsymbol{\theta}_{plc})}{\partial \boldsymbol{\theta}_{plc}} \quad (13)$$

Next, to apply the REINFORCE algorithm, we substitute the gradient of the  $\mathcal{L}_{hrd}$  for a sampled trajectory in Eq. (13) with the gradient of the expected  $\mathcal{L}_{hrd}$  for multiple sampled trajectories as

$$\frac{1}{B} \sum_{i=1}^B \frac{\partial \mathbb{E}_{t \in T} \mathcal{L}_{hrd}^{(t)}(\mathbf{x}_i; \boldsymbol{\theta}_{plc})}{\partial \boldsymbol{\theta}_{plc}} \quad (14)$$

By applying the REINFORCE algorithm, we have (batch averaging is omitted for simplicity)

$$\frac{\partial \mathbb{E}_{t \in T} \mathcal{L}_{hrd}^{(t)}(\mathbf{x}_i; \boldsymbol{\theta}_{plc})}{\partial \boldsymbol{\theta}_{plc}} = \frac{\partial \sum_{t=1}^T \mathcal{P}_{(t)}(\mathbf{x}_i; \boldsymbol{\theta}_{plc}) \mathcal{L}_{hrd}^{(t)}(\mathbf{x}_i; \boldsymbol{\theta}_{plc})}{\partial \boldsymbol{\theta}_{plc}} \quad (15)$$

$$= \sum_{t=1}^T \frac{\partial \mathcal{P}_{(t)}(\mathbf{x}_i; \boldsymbol{\theta}_{plc})}{\partial \boldsymbol{\theta}_{plc}} \mathcal{L}_{hrd}^{(t)}(\mathbf{x}_i; \boldsymbol{\theta}_{plc}) \quad (16)$$

$$= \sum_{t=1}^T \mathcal{P}_{(t)}(\mathbf{x}_i; \boldsymbol{\theta}_{plc}) \frac{\partial \log(\mathcal{P}_{(t)}(\mathbf{x}_i; \boldsymbol{\theta}_{plc}))}{\partial \boldsymbol{\theta}_{plc}} \mathcal{L}_{hrd}^{(t)}(\mathbf{x}_i; \boldsymbol{\theta}_{plc}) \quad (17)$$

$$= \mathbb{E}_{i \in T} \frac{\partial \log(\mathcal{P}_{(t)}(\mathbf{x}_i; \boldsymbol{\theta}_{plc}))}{\partial \boldsymbol{\theta}_{plc}} \mathcal{L}_{hrd}^{(t)}(\mathbf{x}_i; \boldsymbol{\theta}_{plc}) \quad (18)$$

$\mathcal{P}_{(t)}(\mathbf{x}_i; \boldsymbol{\theta}_{plc})$  is the probability of sampled trajectory. Following the previous practices [19, 26, 48], we approximate Eq. (18) as

$$\frac{\partial \mathbb{E}_{t \in T} \mathcal{L}_{hrd}^{(t)}(\mathbf{x}_i; \boldsymbol{\theta}_{plc})}{\partial \boldsymbol{\theta}_{plc}} \approx \frac{1}{T} \sum_{t=1}^T \frac{\partial \log(\mathcal{P}_{(t)}(\mathbf{x}_i; \boldsymbol{\theta}_{plc}))}{\partial \boldsymbol{\theta}_{plc}} \mathcal{L}_{hrd}^{(t)}(\mathbf{x}_i; \boldsymbol{\theta}_{plc}) \quad (19)$$

Next, by expanding  $\mathcal{P}_{(t)} = \prod_{h=1}^H p_{(t)}^h$ , we have

$$\frac{\partial \mathbb{E}_{t \in T} \mathcal{L}_{hrd}^{(t)}(\mathbf{x}_i; \boldsymbol{\theta}_{plc})}{\partial \boldsymbol{\theta}_{plc}} \approx \frac{1}{T} \sum_{t=1}^T \frac{\partial \log(\prod_{h=1}^H p_{(t)}^h(\mathbf{x}_i; \boldsymbol{\theta}_{plc}))}{\partial \boldsymbol{\theta}_{plc}} \mathcal{L}_{hrd}^{(t)}(\mathbf{x}_i; \boldsymbol{\theta}_{plc}) \quad (20)$$

$$\approx \frac{1}{T} \sum_{t=1}^T \frac{\partial \sum_{h=1}^H \log(p_{(t)}^h(\mathbf{x}_i; \boldsymbol{\theta}_{plc}))}{\partial \boldsymbol{\theta}_{plc}} \mathcal{L}_{hrd}^{(t)}(\mathbf{x}_i; \boldsymbol{\theta}_{plc}) \quad (21)$$

$$\approx \frac{1}{T} \sum_{t=1}^T \sum_{h=1}^H \frac{\partial \log(p_{(t)}^h(\mathbf{x}_i; \boldsymbol{\theta}_{plc}))}{\partial \boldsymbol{\theta}_{plc}} \mathcal{L}_{hrd}^{(t)}(\mathbf{x}_i; \boldsymbol{\theta}_{plc}) \quad (22)$$

To reduce the variance of gradient estimation, we apply the baseline trick by subtracting mean value,  $\tilde{\mathcal{L}}_{hrd} = \frac{1}{T} \sum_{t=1}^T \mathcal{L}_{hrd}^{(t)}(\mathbf{x}_i; \boldsymbol{\theta}_{plc})$ , from  $\mathcal{L}_{hrd}^{(t)}$  as

$$\frac{\partial \mathbb{E}_{t \in T} \mathcal{L}_{hrd}^{(t)}(\mathbf{x}_i; \boldsymbol{\theta}_{plc})}{\partial \boldsymbol{\theta}_{plc}} \approx \frac{1}{T} \sum_{t=1}^T \sum_{h=1}^H \frac{\partial \log(p_{(t)}^h(\mathbf{x}_i; \boldsymbol{\theta}_{plc}))}{\partial \boldsymbol{\theta}_{plc}} [\mathcal{L}_{hrd}^{(t)}(\mathbf{x}_i; \boldsymbol{\theta}_{plc}) - \tilde{\mathcal{L}}_{hrd}] \quad (23)$$

Eventually, by adding back the batch averaging, we have our ultimate form of gradients as

$$\frac{\partial \mathbb{E}_{i \in B} \mathbb{E}_{t \in T} \mathcal{L}_{hrd}^{(t)}(\mathbf{x}_i; \boldsymbol{\theta}_{plc})}{\partial \boldsymbol{\theta}_{plc}} \approx \frac{1}{B \cdot T} \sum_{i=1}^B \sum_{t=1}^T \sum_{h=1}^H \frac{\partial \log(p_{(t)}^h(\mathbf{x}_i; \boldsymbol{\theta}_{plc}))}{\partial \boldsymbol{\theta}_{plc}} [\mathcal{L}_{hrd}^{(t)}(\mathbf{x}_i; \boldsymbol{\theta}_{plc}) - \tilde{\mathcal{L}}_{hrd}] \quad (24)$$

## C Experiment Setting

**General training settings.** For CIFAR10, models were trained by stochastic gradient descent (SGD) for 200 epochs with an initial learning rate 0.1 divided by 10 at 50% and 75% of epochs. The momentum was 0.9, the weight decay was 5e-4 and the batch size was 128. The experiments on Imagenette and SVHN followed a similar protocol as those on CIFAR10 except the following changes. The initial learning rate on SVHN was 0.01. For Imagenette, the weight decay was 1e-4, the total number of epochs was 40, and the learning rate was decayed at 36th and 38th epoch. The ViT-B/16 was pre-trained on ImageNet-1K [8]. Gradient clipping was applied throughout training. Experiments were run on Tesla V100 and A100. All results reported by us were averaged over 3 runs.

**Adversarial training settings.** For AT, we used  $\ell_\infty$  projected gradient descent [28] with a perturbation budget,  $\epsilon$ , of 8/255. The number of steps was 10 and the step size was 2/255 for CIFAR10 and 1/255 for SVHN. To stabilize the training on SVHN, the perturbation budget,  $\epsilon$ , was increased

Table 7: The value of hyperparameters of our method used in various training settings. The value of  $l$  and  $u$  listed here is a factor relative to the arithmetic mean chance,  $\tilde{p}$ , of sampling an augmentation in each group (prediction head), so the real absolute threshold value will be, e.g.,  $l \cdot \tilde{p}$ . Taking an example of the Crop prediction head with 16 (1+15) magnitudes in total,  $\tilde{p} = 1/16$ . Hyperparameters are optimized using grid search.

	CIFAR10		Imagenette	SVHN
Model	WRN34-10	WRN34-10	ViT-B/16	PRN18
Training	AT(-SWA)	AT-AWP(-SWA)	AT	AT
Policy backbone	PRN18	PRN18	ViT-B/16	PRN18
Affinity model	WRN34-10	WRN34-10	ViT-B/16	PRN18
$\lambda$	0.4, 0.2, 0.1	0.7 0.5 0.4	0.3	0.01
$\beta$	0.8	0.8	0.8	0.3
Diversity limits ( $l, u$ )	(0.9, 4.0)	(0.9, 4.0)	(0.8, 4.0)	(0.7, 4.0)
Policy learning rate	0.001	0.001	0.1	0.001

from 0 to 8/255 linearly in the first five epochs and then kept constant for the remaining epochs, as suggested by [2]. Note that, following [34], we tracked PGD10 robustness on the test set at the end of each epoch during training and selected the checkpoint with the highest PGD10 robustness, i.e., the "best" checkpoint to report robustness.

**Configuration of AROID.** Vulnerability objective was calculated based on PGD2 with a step size of 2/255. The affinity models used the same architecture as the target model. The affinity models were pre-trained using standard training with the same settings as their AT trained counterparts yet with no augmentation. Early stopping was used if training accuracy was close to 100%. The policy model’s backbone was PRN18 on CIFAR10 and SVHN, and ViT-B/16 (pre-trained on ImageNet-1K) on Imagenette as it was observed to be difficult for PRN18 to quickly fit Imagenette data to a reasonable degree in standard training. Note that this ability is especially important when training on Imagenette because the total number of epochs (40) is much less than for the other datasets (200). The policy model was trained using SGD with a constant learning rate (0.001 for CIFAR10 and SVHN and 0.1 for Imagenette due to the reduced number of training epochs) and the same momentum as the target optimizer’s. Gradient clipping was applied to stabilize the training of the policy model. In the initial five epochs of training, we did not train the policy model nor apply it to augment the data (no augmentation at all was applied) since the target model changed rapidly. When training on CIFAR10, we progressively hardened DA by decreasing  $\lambda$  as the learning rate decayed since this improved robustness over the constant  $\lambda$  scheme. The value of main hyperparameters used in our experiments are summarized in Tab. 7.

**Configuration of compared DA methods.** AutoAugment was parameterized as in [6] since we did not have sufficient resource to optimize. For AutoAugment, augmentations were applied in the order of HorizontalFlip-RandomCrop-AutoAugment-Cutout (16x16) on CIFAR10 and Imagenette, and AutoAugment-Cutout (20x20) on SVHN, as in [6]. TrivialAugment is parameter-free so no tuning was needed. For TrivialAugment, augmentations were applied in the order of HorizontalFlip-RandomCrop-TrivialAugment-Cutout (16x16) on CIFAR10 and Imagenette, and TrivialAugment-Cutout (16x16) on SVHN, as in [31]. For Cutmix,  $\alpha = 0.25$  and  $\beta = 1$  on CIFAR10 as optimized in [23];  $\alpha = 1$  and  $\beta = 1$  on Imagenette and SVHN as suggested in [45]. For Cutout, the size of cut-out area was 20x20 on all three datasets as in [23]. Cutout and Cutmix were applied with the default (baseline) augmentations in the order of HorizontalFlip-RandomCrop-Cutout and -Cutmix respectively on CIFAR10 and Imagenette, while no additional augmentations were applied on SVHN. For IDBH, IDBH[strong]-CIFAR10 was used on CIFAR10 and Imagenette, and IDBH-SVHN was used on SVHN.

**Configuration of compared state-of-the-art robust training methods.** We only re-implemented the algorithms of SWA and AWP to report the result based on our runs, while the result of the others including MART, MART-AWP, SEAT, LAT-AT and LAS-AWP were copied directly from their original works except that the result of MART was copied from [43] for a better aligned training setting. SWA was implemented as in [33] with a decay rate of  $\tau = 0.999$ . AWP was configured as in

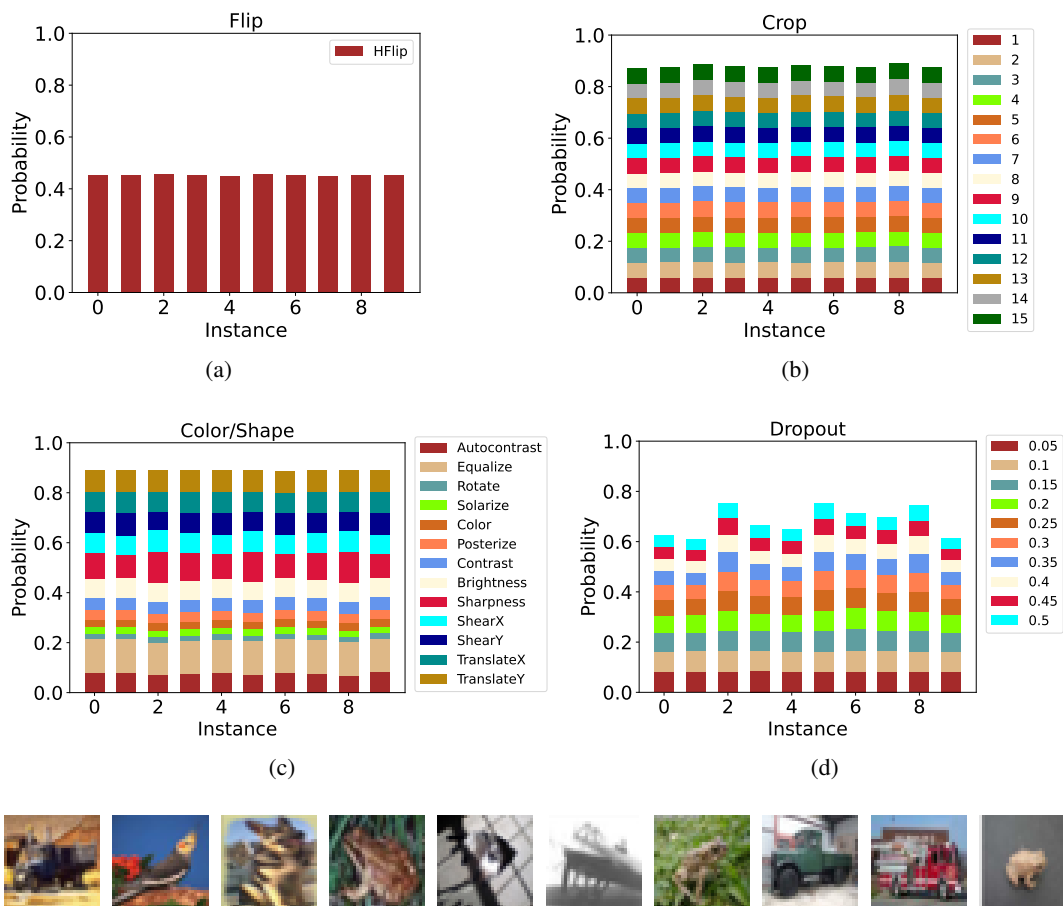


Figure 5: Visualization of the learned DA policies, applied to ten images randomly sampled from CIFAR10 training set, for the Flip, Crop, Color/Shape and Dropout types of augmentations. The policy model is resumed from a checkpoint saved at the end of 110<sup>th</sup> epoch, which is randomly sampled from 200 epochs, i.e., a course of training a WRN34-10 model on CIFAR10 (following the training setting as specified in Appendix C). The sampled ten images are visualized at the bottom in an order of x-axis in the above figures. The chance of applying no transformation (Identity) is the gap between the colored bar and the top (i.e., score of 1.0). In the Color/Shape group, the probabilities of different magnitudes are not shown separately, but are summed to get the overall probability of a transformation.

[43] with  $\beta = 0.005$ . Note that the same configurations of SWA and AWP were used to train with baseline DA and AROID.

## D Visualization of Learned DA policies

Fig. 5 visualizes the learned distribution of DAs for different, randomly sampled, data instances. Instance-wise variation of the learned DA policy is visible for the Color/Shape augmentations (Fig. 5c) and evident for the Dropout augmentations (Fig. 5d), but subtle in the rest (Fig. 5a and Fig. 5b). Note that even for the different data instances from the same class (e.g., instances 4, 7, 10 from the class "frog"), the learned DA distributions can still differ considerably (Fig. 5d). This confirms that (1) AROID is able to capture and meet the varied demand of augmentations from different data instances, and (2) such demand exists for some, but not all, augmentations. These observations may explain why many instance-agnostic DA methods such as IDBH, despite being inferior to ours, still work reasonably well (see Tab. 1).



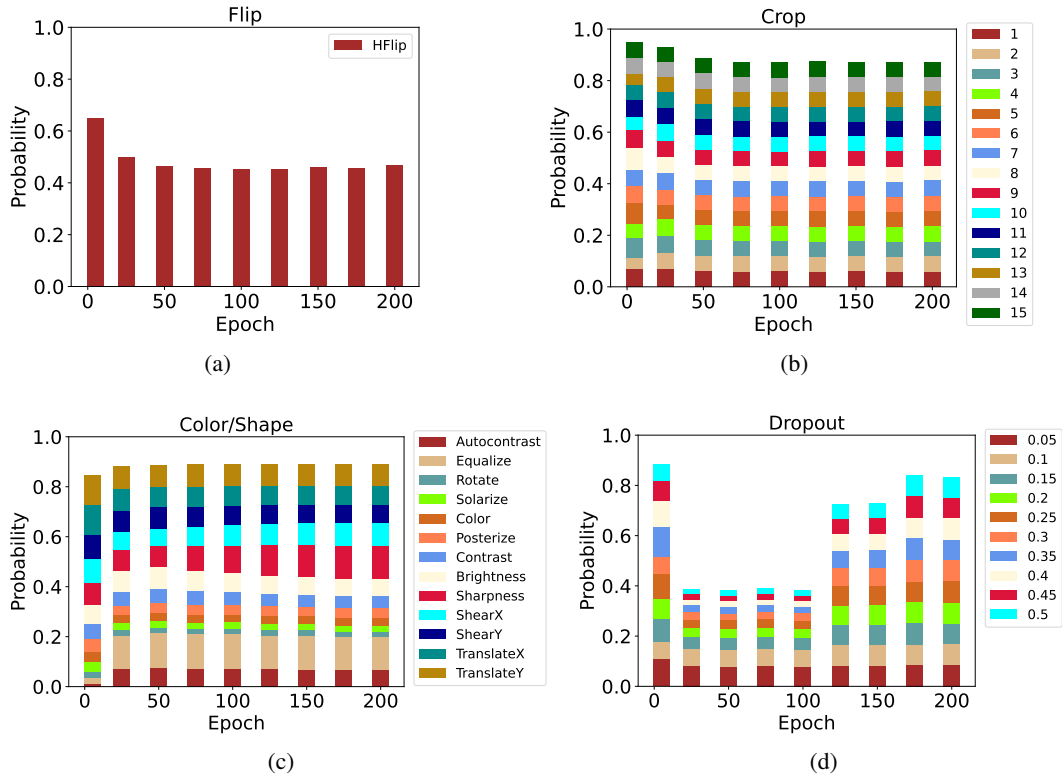


Figure 6: Visualization of how the learned DA policies evolve as training progresses. The same, randomly sampled, image (visualized at the bottom) was used across epochs (5, 25, 50, 75, 100, 125, 150, 175, 200) to produce the policies. The first bar in each sub-figure corresponding to the epoch 5 describes the initial status of the policy model (recalling that the training of policy model starts from epoch 5). For each bar in the figures, the policy model was resumed from the checkpoint saved at the corresponding epoch (x-axis) in the same course of training. The chance of applying no transformation (Identity) is the gap between the colored bar and the top (i.e., the score of 1.0). In the Color/Shape group, the probabilities of different magnitudes are not shown separately, but are summed to get the overall probability of a transformation.

It was also observed in Fig. 6 that the learned DA policy for the same data instance evolved as training progressed. In the Color/Shape group (Fig. 6c), augmentations like Sharpness became observably more likely to be selected while others such as ShearY became less probable as training continued. Dropout (i.e. Erasing; Fig. 6d) particularly with large magnitudes was rarely applied prior to 100th epoch, i.e., the first decay of learning rate. The possibility of applying Crop (i.e. Cropshift; Fig. 6b) and Flip (i.e. HorizontalFlip; Fig. 6a) first dropped until the first decay of learning rate and then stayed nearly constant afterwards.

Consistent to the previous findings on standard training [6] and harmful augmentations [33], we observed that AT on CIFAR10 favored mostly color-based augmentations like Equalize and Sharpness and disfavored geometric augmentations like Rotate and harmful augmentations like Solarize and Posterize (see both Fig. 5c and Fig. 6c). This verifies the effectiveness of our DA policy learning algorithm.